Rotorcraft Low Noise Trajectory Design: a focus on RACER

Pierre Dieumegard, Frédéric Guntzer, Julien Caillet

Rotorcraft Low Noise Trajectory Design: a focus on RACER

Pierre Dieumegard[1,2], Frédéric Guntzer[1], Julien Caillet[1]

[1] Airbus Helicopters
Aéroport Marseille Provence, 13725 Marignane Cedex - France
[2] Ecole Nationale de l'Aviation Civile, Université de Toulouse
7 Avenue Edouard Belin, 31055 Toulouse Cedex 4 - France
{pierre.p.dieumegard,frederic.guntzer,julien.caillet}@airbus.com

ABSTRACT

Aviation is heading towards more sustainability. In this context, this paper proposes a methodology to design low noise trajectories for rotary-wing aircraft. A dedicated algorithmic scheme is presented, embedding Airbus Helicopters internal noise footprint computation chain. This software is able to accurately model rotorcraft noise emission, and perform realistic impact assessment on population. The proposed optimization method has been tested on several real-world instances, predicting notable noise reductions by flying such optimized low noise procedures. Furthermore, additional acoustic gains can be obtained thanks to a supplementary degree of freedom brought by a new innovative rotorcraft configuration.

INTRODUCTION

In order to reach more sustainability, aviation needs to reduce its global emissions. Among them, great emphasis has been placed on reducing CO_2, NOx and other greenhouse gases emissions to limit the impact of aviation on climate change. Some reductions can already be achieved by using greener fuels such as Sustainable Aviation Fuels (SAF) on current aircraft. In addition, new propulsion means and aircraft conceptual designs should bring even more sustainability in the coming years.

Furthermore, the expected growth in aircraft, especially rotorcraft, operations above cities with the emergence of Urban Air Mobility (UAM) comes with another type of emission that can also have severe health impact: noise. The World Health Organization (WHO) has recently published a report containing recommendations for protecting human health from exposure to global environmental noise in the European region [1]. Regarding aircraft noise, the WHO strongly recommends to reduce global noise levels produced by aircraft below 45dB L_{den}, and even 40dB L_{night} for noise levels produced by aircraft during night time (11:00PM - 7:00AM) [1]. Such recommendations might be enforced as domestic regulatory policies in some European countries in the coming years. As most of air operations in sensitive areas are conducted by rotorcraft, it has become essential to lower rotorcraft noise emissions in order to comply with the WHO recommendations and to improve community acceptance.

There are two main ways to reduce rotorcraft global noise. On the one side, noise abatement can be achieved by modifying the design/architecture of the rotorcraft [2, 3]. On the other side, the operational noise can be reduced by flying quietly along low-noise optimal trajectories [4–8].

The paper is structured as follows. The first section details the general mechanism of rotorcraft operational noise. The second section introduces the recent capability to perform realistic noise impact assessment of rotorcraft traffic. The third section presents a new method to compute low-noise optimal trajectories and associated numerical results are given on real-world scenarios. Finally, the last section describes the specific design characteristics and the expected advantages brought by a new rotorcraft configuration: the Rapid And Cost-Effective Rotorcraft (RACER).

ROTORCRAFT NOISE: GENERALITIES

The sound emitted by a rotorcraft is very complex since it comes from various sources. Among them, the high levels of harmonic rotor noise are often associated with strong annoyance. Blade-Vortex Interaction (BVI) is one mechanism that generates such high level impulsive noise and is considered indeed as one of the most annoying rotorcraft noise sources. It is thus essential to limit/avoid the generation of BVI noise in order to broaden public acceptance of rotorcraft and ensure more sustainable operations.

BVI noise is generated by the interaction between the rotor blade and the tip vortices shed from the preceding blades. In steady level flight, the tip vortices tend to be convected below the rotor plane due to the induced velocity through the rotor disk, as represented in Figure 1a. In descending flight, the presence of the upward inflow forces the tip vortices to be convected in the plane of the rotor, as depicted in Figure 1b. The

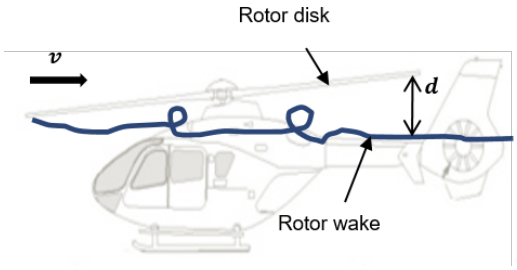

(a) Level flight. The wake is convected below the rotor disk with miss-distance d.

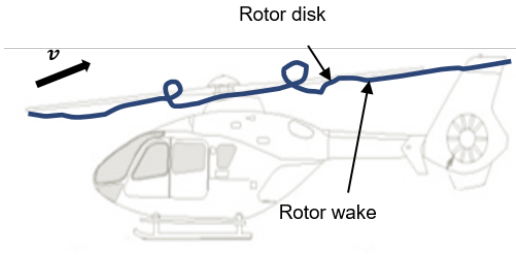

(b) Descending flight. The wake is convected in the rotor disk plane.

Figure 1: BVI geometry in the vertical plane.

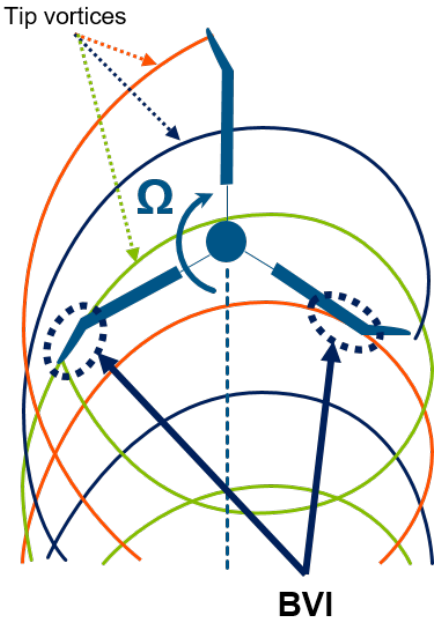

Figure 2: BVI geometry in the rotor plane. Strong parallel interaction on the advancing blade side (left).

interactions between the tip vortices and the blades cause large blade loads variations, resulting in high level noise peaks. BVI noise is thus predominant during descending flight, with noise peaks occurring near the standard 6° flight path angle and for typical approach speeds, as shown in Figure 5.

Previous theoretical and experimental researches [9–11] have shown that rotor noise radiation in steady-state flight, and especially BVI noise, are governed by a finite set of flight parameters: the thrust coefficient (C_T), the rotor advance ratio (μ) and the tip-path-plane angle of attack (α_{TPP}). The thrust coefficient (C_T) controls the rotor blade loading. In particular, it controls the strength and the size of the tip vortices, hence the strength of BVI noise. The rotor advance ratio (μ) controls the motion of the blade. In particular, it controls the epicycloidal pattern of the wake and hence the geometry of the BVI in the rotor disk plane. BVI can both occur in the advancing and retreating blade side, as illustrated in Figure 2. The more parallel the interaction, the stronger the resulting BVI noise. In addition, μ and α_{TPP} control the geometry of the BVI in the vertical plane through the spacing between the rotor blades and the tip vortices, also called *miss-distance (d)*, represented in Figure 1a. The smaller the miss-distance, the closer the rotor blades to their wake, the stronger the interaction, and hence the higher the resulting noise peaks.

In this paper, we assume that gross weight and rotor RPM are held constant. Under these assumptions and in steady-state flight, C_T remains constant and μ depends only on the rotorcraft airspeed (v). The longitudinal force balance, represented in Figure 3, can also be simplified to the following expression:

$$\alpha_{TPP} = -\frac{D_f + H}{W} - \gamma - \frac{1}{W}\frac{\mathrm{d}v}{\mathrm{d}t}$$

Under the same assumptions, the fuselage drag (D_f) and the rotor "hub-force" (H) depends mainly on the helicopter airspeed (v). Therefore in steady-state flight ($\frac{\mathrm{d}v}{\mathrm{d}t} = 0$), α_{TPP} is totally governed by v and the flight path angle (γ). v and γ are indeed widely used in literature as noise governing parameters [4–6]. In addition, to handle non-steady flight conditions, an acoustic equivalence is usually made between moderate acceleration/deceleration and an effective flight path angle [5,12]. Figure 5 shows an aeroacoustic database for the H130 helicopter. We observe that the emitted noise can vary up to 10 dB(A) depending on the helicopter flight condition (v,γ). In particular, the BVI noise region is clearly identifiable around standard descending flight condition ($v = 70$ kt, $\gamma = -6°$).

In the scope of getting more sustainable rotorcraft operations, we must find quieter ways to fly. For conventional helicopters, the main rotor ensures all the lift and propulsion. It has been shown previously that, in this case, the value of the main rotor tip-path-plane angle of attack (α_{TPP}) is imposed by the helicopter flight condition (v,γ). As a consequence, flying quietly is possible only by defining trajectories where helicopters avoid the noisiest (v,γ) flight conditions, and especially the BVI region. Such trajectories are called noise abatement trajectories and their computation is detailed

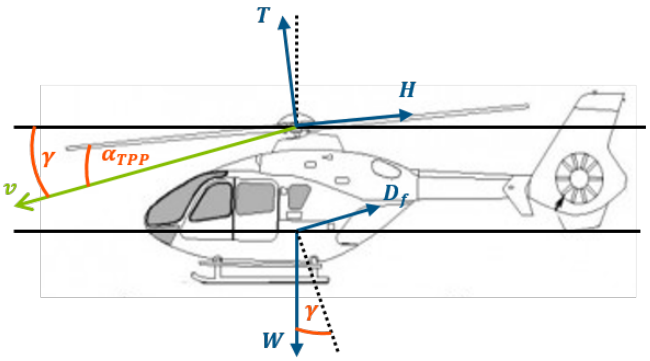

Figure 3: Longitudinal force balance of a classical helicopter.

in the following.

ENVIRONMENTAL IMPACT ASSESSMENT

In order to compute optimal noise abatement trajectories, one needs a tool to evaluate and compare each candidate trajectory. The software tool considered in this paper is the Airbus Helicopters internal noise footprint computational chain: CAROT (Compute Acoustics of a Rotorcraft Over Terrain). It relies on several aeroacoustic databases, which are specific to each aircraft type (e.g. EC120, H130, H135, H145, H155...) and which have been built from dedicated flight test measurement campaigns. Each database contains the noise emitted by the associated rotorcraft type as a function of the flight condition (v,γ). The noise information is provided in the form of a hemisphere in order to account for the specific directivities of rotorcraft noise. An illustration of a hemisphere for the noise radiated by a H130 helicopter in typical cruise flight condition (v = 110 kt, $\gamma = 0°$) is given as an example in Figure 4. A representation of the complete noise emission database for the H130 helicopter is given in Figure 5.

Such noise database is then coupled to a trajectory generator to compute the noise emitted by the rotorcraft throughout the trajectory. Finally, a comprehensive noise propagation model is applied to estimate the noise perceived at different observer locations on the ground. More details about the functioning of the software tool can be found in [5] and [8].

Besides performing an accurate and efficient computation of rotorcraft noise footprint, the computational chain has recently been adapted to be able to handle geo-referenced data [8]. This was an essential prerequisite for the coupling with environmental data. The new simulation environment is now based on the ICAO standard World Geodetic System 1984 (WGS84) and takes into account the curvature of the Earth. The

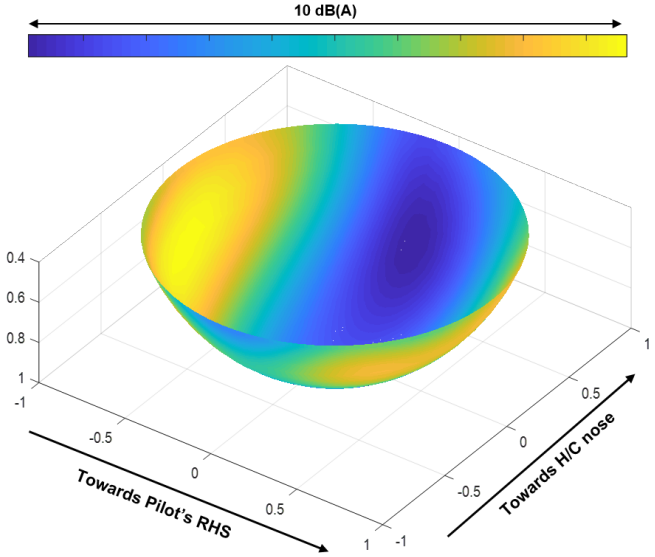

Figure 4: Hemisphere representation of the H130 helicopter noise radiated in level flight (v = 110 kt, $\gamma = 0°$).

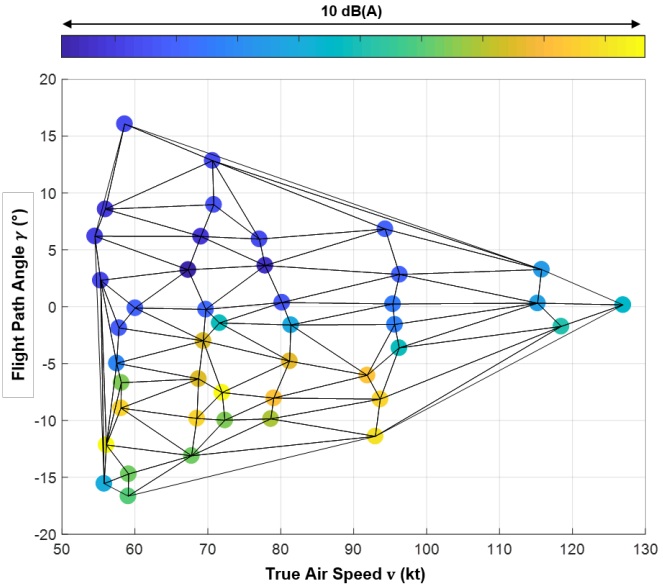

Figure 5: Aeroacoustic database representation for the H130 helicopter. Colored dots represent the radiated noise according to various flight conditions (v,γ): the yellower, the noisier.

coupling of the tool with several environmental data and their respective interest are introduced in the following. All the examples given hereafter refer to rotorcraft traffic in different geographical areas in France.

Real-world traffic data

Since it can handle geo-referenced data, the software tool considered in this paper is able to assess the noise footprint of real rotorcraft traffic data. This capability

is essential to better understand community response to rotorcraft operations, which is a first step to go for more sustainability.

There are multiple ways to access aircraft traffic data as they are more and more available. In this paper, we use a mix of traffic data coming from Automatic Dependent Surveillance Broadcast (ADS-B) data, radar data in the vicinity of heliports and trajectory data recorded by rotorcraft avionics. The *real* noise footprint associated with the trajectories that have been really flown can be computed by the previously described software tool. This allows to compare the *real* impact of rotorcraft operations to their hypothetical impact, which is computed according to the trajectories published in the different aeronautical charts, such as the Visual Approach Charts (VACs) in the vicinity of heliports. Figure 6 shows an example of such a comparison for the approach to Cannes heliport. We can see significant differences between both trajectories, and accordingly between their associated noise footprints. In particular, we observe that the really-flown trajectory passes closer to the coast than the reference one, leading to a potential increase in the associated noise annoyance.

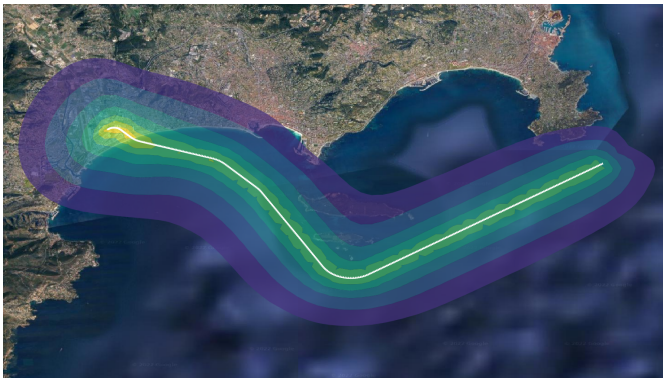

(a) Noise footprint of the published approach procedure (in white) to Cannes heliport, defined according to the VAC.

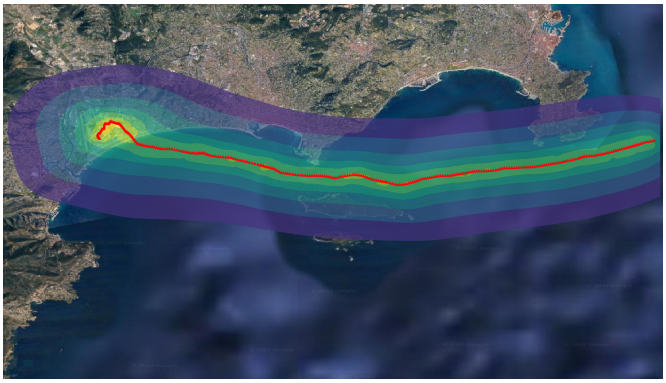

(b) Noise footprint of a really-flown approach trajectory (in red) to Cannes heliport. This trajectory has been extracted from radar traffic data for the day of July 29$^{\text{th}}$, 2019.

Figure 6: Comparison of Sound Exposure Level (SEL) 5 dB(A) contours between published and real approach trajectories to Cannes heliport (ICAO code: LFMD).

The differences between published trajectories and what is really flown shows that there is a need to update the recommended trajectories in order to get more quiet and sustainable rotorcraft operations.

Elevation data

The capability to handle geo-referenced data allows the tool to also take into account terrain elevation data in the definition of the set of ground locations where the noise levels are computed. This is much more realistic than considering a flat ground, especially when assessing the noise footprint of rotorcraft operations in mountainous areas. It might indeed significantly affect the sound propagation distance, whose role is twofold in the noise attenuation. In this paper, the digital elevation model considered if Digital Terrain Elevation Data (DTED level 1). More details can be found in [8].

Demography

Heading towards more sustainability comprises improving public acceptance of rotorcraft operations. As this challenge is people-centred, it is essential for the software tool to be coupled with demographic data. In this paper, we rely on publicly available demographic data from the French National Institute of Statistics and Economic Studies (INSEE). Thanks to such coupling, not only raw noise levels are computed on the ground, but more extensive analyses can be conducted. In particular, the impact of rotorcraft operations on population can be assessed through the computation of various noise indicators. As an example, for the scenario considered in Figure 6, the really-flown trajectory (plotted in red) is associated with a 32% increase in the number of people impacted by a maximum A-weighted level ($L_{A,max}$) above 75 dB(A). Further details about the coupling are provided in [8].

Demographic data are essential for local players to better understand community response by correlating the complaints to the *real* noise impact on population. Furthermore, they will be useful in the frame of low-noise trajectory design. Optimization can thus be focused on the minimization of population exposure to noise rather than the reduction of noise contours areas.

Background noise

The software tool has also been coupled to background (ambient) noise data. It is indeed known that noise annoyance strongly depends on the observer surrounding environment. Therefore, considering background noise is an additional asset to better understand community response to rotorcraft operations. In this paper, we use background noise data from BruitParif that is available for the Paris region only [13]. Figure 7a shows a representation of background noise data in the Paris

region. We remark that roads and railways are clearly identifiable as noisy sources. Additional information about the coupling of the tool with ambient noise data is available in [8].

Thanks to this coupling, rotorcraft noise emergence above ambient noise can be computed and integrated in the optimization process. Noise emergence is defined as the difference between the $L_{A,max}$ value generated by the rotorcraft and the $L_{A,eq}$ value of background noise. An illustration of rotorcraft noise emergence is given in Figure 7b for a single approach flight to Issy-les-Moulineaux heliport.

The coupling of the software tool with all the above-mentioned environmental data allows to perform realistic environmental impact assessment of rotorcraft operations. This is essential to better understand community response, which is the first step towards improving sustainability. In addition, such environmental data allows to define a dedicated indicator representing population exposure to rotorcraft noise, which can further be used within optimization. The definition of the indicator and the method to compute optimized low-noise rotorcraft trajectories are detailed in the next section.

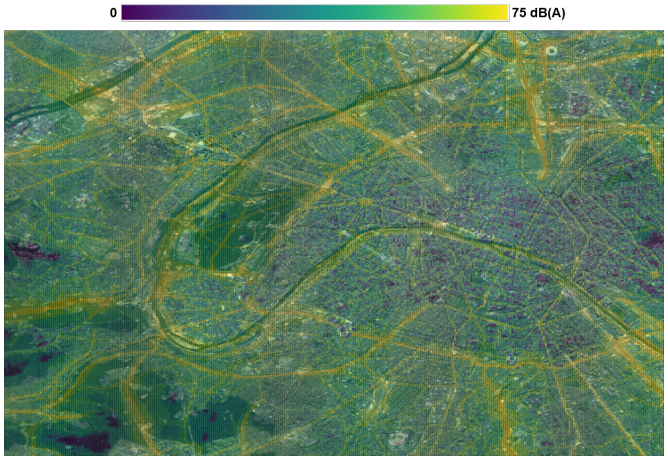

(a) Background noise in Paris region around Issy-les-Moulineaux heliport.

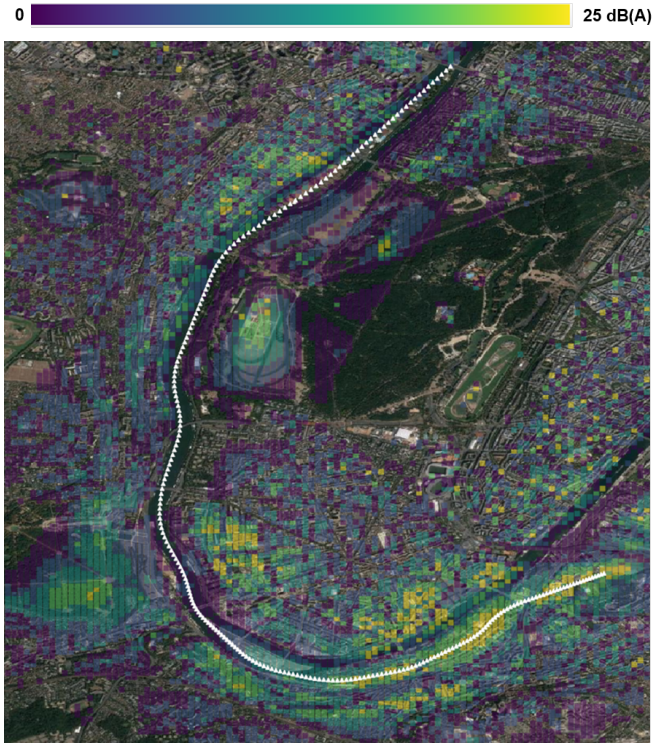

(b) Rotorcraft noise emergence above background noise for a typical approach trajectory (in white) to Issy-les-Moulineaux heliport.

Figure 7: Background noise data and rotorcraft noise emergence in the vicinity of Issy-les-Moulineaux heliport (ICAO code: LFPI).

ROTORCRAFT TRAJECTORY OPTIMIZATION

Aviation is heading towards more sustainability. In this frame, this paper focuses on reducing the noise annoyance due to rotorcraft operations to improve public acceptance. This objective can be achieved by flying more quietly along noise abatement trajectories. The problem of computing such optimized trajectories is addressed as a trajectory optimization problem, which is detailed in the following.

Cost function

The objective is to minimize population exposure to rotorcraft noise. The definition of the cost function f to be minimized is detailed hereafter. Let N_m be the number of observer locations, where the noise level has been computed. For all $k \in \{1, 2, \ldots, N_m\}$, let SEL($k$) and p_k respectively be the Sound Exposure Level (SEL) and the number of people associated with location k. The total population considered for the impact assessment of a given trajectory is defined as follows:

$$p_{tot} = \sum_{\substack{k \in [1, N_m]: \\ \mathrm{SEL}(k) \geq \mathcal{L}_{thr}}} p_k \tag{1}$$

where $\mathcal{L}_{thr}$ is the user-defined threshold of SEL values to be considered, expressed in dB(A). As an example, in this paper, we use $\mathcal{L}_{thr} = 70$ dB(A). The according set of relevant SEL values is then defined as:

$$\mathcal{L} = \{\mathcal{L}_{thr}, \mathcal{L}_{thr} + 5, \mathcal{L}_{thr} + 10, \ldots, 100\}\mathrm{dB(A)} \tag{2}$$

For all $i \in \{1, 2, \ldots, |\mathcal{L}|\}$, let $\mathcal{M}_i$ be the subset of observer locations, whose SEL value is in $[\mathcal{L}_i, \mathcal{L}_{i+1}[$:

$$\mathcal{M}_i = \{k \in [1, N_m], \mathcal{L}_i \leq \mathrm{SEL}(k) < \mathcal{L}_{i+1}\}. \tag{3}$$

Finally, the cost function f considered in this paper is defined as the weighted sum of the population impacted by the different SEL values generated by a given

rotorcraft trajectory. The expression of f is given below:

$$f = \sum_{i=1}^{|\mathcal{L}|} \left(\alpha_i \cdot \sum_{k \in \mathcal{M}_i} \frac{p_k}{p_{tot}} \right) \quad (4)$$

where the choice of the weighting factors $\alpha_i \geq 1, i \in \{1, 2, \ldots, |\mathcal{L}|\}$ is let to the user to give more or less weight to the different SEL values.

Solution algorithm

This objective function is then embedded in a dedicated algorithmic scheme to compute optimal noise abatement trajectories. From the optimization perspective, the problem belongs to the class of Black-Box Optimization (BBO) problems. Indeed, due to the complex treatments performed by CAROT during the evaluation of one trajectory candidate, there are no complete analytical expression of the objective function in terms of the decision variables. Therefore, the algorithmic scheme relies on a state-of-the-art method, which is known to be efficient for solving BBO problems: the Mesh Adaptive Direct Search (MADS) algorithm [14]. As it is a local method, a good initial trajectory candidate is provided as the result of an auxiliary simplified path planning problem, which is solved by the Fast Marching Tree method (FMT*) [15]. Then, MADS is applied to search for a locally optimal trajectory lying within a corridor defined around such initial trajectory candidate. A schematic view of the algorithm is given in Figure 8. More details about the functioning of the algorithmic scheme can be found in [8, 16].

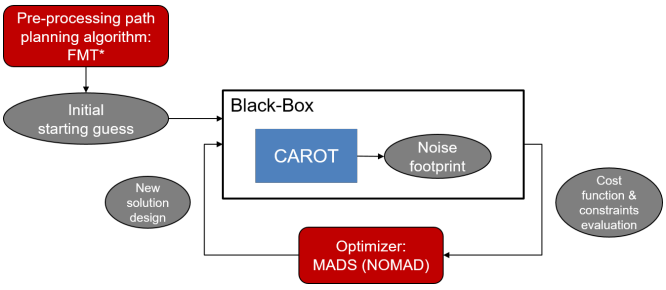

Figure 8: Diagram of the proposed algorithmic scheme.

Numerical results

In this section, we present the numerical results from several test cases that have been performed on a Linux platform with 48 CPUs (3.0 GHz) and 130 GB RAM. We focus on one representative instance, that corresponds to a cruise and approach flight to a heliport located in a high-densely populated area.

Depending on the local regulations, the 2D lateral path of the trajectory might be fixed. A first test, referred to as *2D Optimal*, considers such an eventuality and focuses on optimizing only the altitude and the speed of the rotorcraft. Figure 9 draws a comparison between the resulting optimal trajectory and a *reference* trajectory, which has been retrieved from radar data. According to Figure 9a, the 2D optimal trajectory comprises a two-steps approach avoiding the typical BVI zone, in particular with a last steep segment (-10°). Significant noise reductions up to 9 dB(A) SEL locally can already be obtained (see Figure 9b).

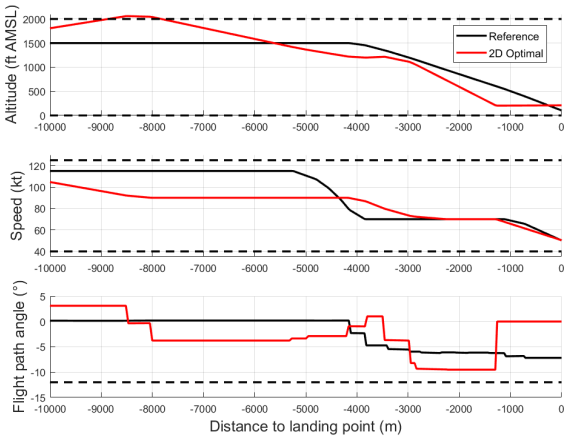

(a) Noise dependant flight parameters profiles.

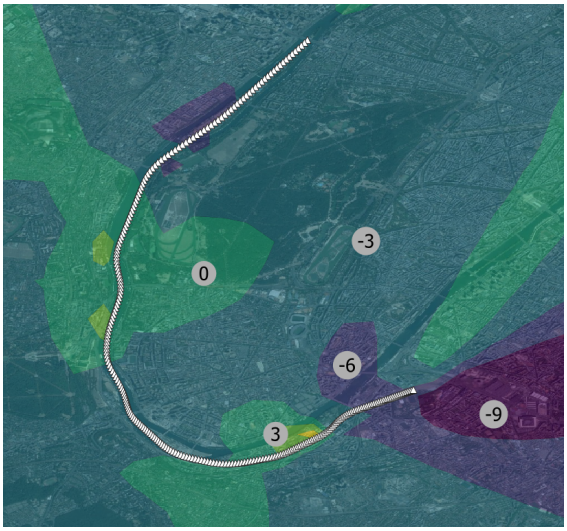

(b) ΔSEL_{2D} = SEL(2D Optimal) - SEL(Reference).

Figure 9: Predicted SEL difference between 2D optimal and reference trajectories and associated flight parameters profiles.

To go further, a second test, referred to as *4D Optimal*, considers the possibility to modify the trajectory in 4D. The new lateral path and vertical profiles are represented in green in Figure 10. Figure 10b shows huge noise reduction (up to -12dB(A) SEL) in comparison to the reference trajectory. We also remark that the

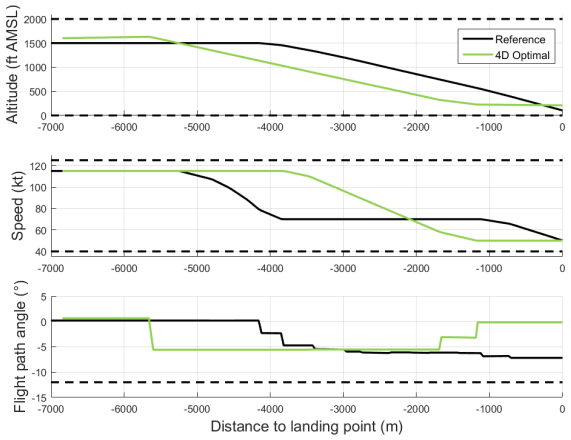

(a) Noise dependant flight parameters profiles.

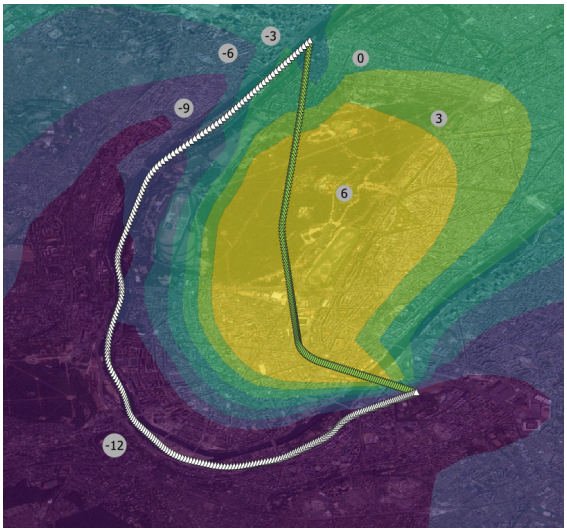

(b) ΔSEL_{4D} = SEL(4D Optimal) - SEL(Reference).

Figure 10: Predicted SEL difference between 4D optimal and reference trajectories and associated flight parameters profiles.

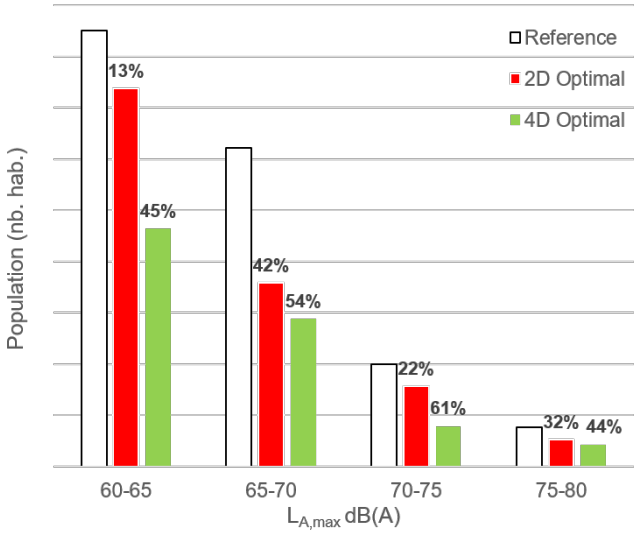

(a) Reduction (%) in population exposure to 5 dB(A) $L_{A,max}$ contours.

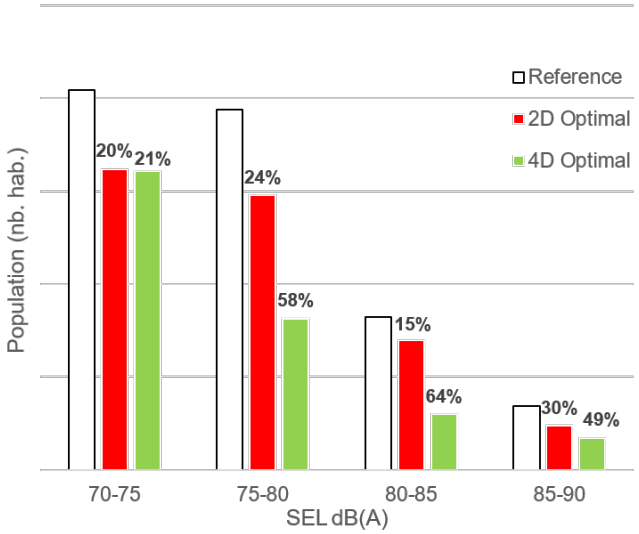

(b) Reduction (%) in population exposure to 5 dB(A) SEL contours.

Figure 11: Predicted gains in the reduction of population exposure to rotorcraft noise for different metrics ($L_{A,max}$, SEL).

modification of the lateral path comes with significant noise increase (up to 6 dB(A) SEL), which remains limited to areas where the population density is lower. Even though these losses, the bar plots in Figure 11 show that a global reduction in the number of people exposed to rotorcraft noise can be achieved for both instantaneous ($L_{A,max}$) and time-integrated (SEL) metrics. The *2D Optimal* trajectory already brings significant reduction of approximately 15 to 40% in the number of people exposed to the different noise contours. Additional reduction up to 20 to 60% can be obtained with the *4D Optimal* trajectory.

Three main effects

According to literature, the significant reduction in population exposure to rotorcraft noise observed in the example presented above is known to be dependent on three main effects that are detailed below.

The first effect is related to the noise emission of the rotorcraft and is referred to as the source effect. Reducing operational noise is indeed achieved by reducing the noise emitted by the rotorcraft. As detailed at the beginning of the paper, this means avoiding the noisy flight conditions, especially the ones causing BVI during the approach phase. In practice, according to the noise emission diagram presented in Figure 5, there are two main ways of avoiding the BVI zone: flying very steep or shallow approaches.

The second effect is related to the geometry of the flight path. Flying high and performing steep approaches allows, by definition, to reduce the noise levels perceived on the ground thanks to the increase in the noise-receiver distance, hence propagation distance. This effect is significant especially undertrack, while it attenuates for an observer placed laterally.

The third effect is related to the ground speed of the rotorcraft trajectory and is referred to as the speed effect. For a given source noise level and a given flight path, the higher the ground speed, the shorter the overflight duration, hence the lower any time-integrated noise metric.

Unfortunately, the second and third effects are counterproductive when considering realistic flyability constraints such as a maximum rate of descent. To comply with such constraint, very steep approaches, which benefit from the second effect must be performed at low speed, which is detrimental to time-integrated noise metrics. It is exactly the other way round for shallow approaches. This contradictions demonstrate that designing low noise trajectories is the result of complex trade-offs, which are determined through the algorithm presented above. However, the results highly depends on the constraints, especially the allowed speed range and maximum rate of descent. More details about the three effects can be found in [5].

The results presented above shows that significant reduction in population exposure to rotorcraft noise can be achieved by flying quieter along optimized trajectories. The biggest reduction can be obtained by modifying the trajectory in 4D (lateral path, altitude and speed profile). However, in some more constrained cases where the lateral path must be kept fixed, some non-negligible reductions can still be achieved, which is consistent with previous researches [4, 5]. The reduction are obtained for both instantaneous ($L_{A,max}$, see Fig. 11a) and time-integrated (SEL, see Fig. 11b) noise metrics showing that the optimizer is able to solve the complex trade-off mentioned above, even though it is limited by the maximum rate of descent allowed. The potential reduction presented in this section remains highly dependent on the instance and the constraints considered.

A NEW ROTORCRAFT CONFIGURATION: RACER

The RACER wing-compound helicopter concept is developed in the frame of the Clean Sky 2 European funded Research Program. Two propellers provide for anti-torque, allowing the removal of the tail anti-torque rotor, as well as for horizontal thrust, allowing a target cruise speed of 220 kt (typically 140 kt for a conventional H/C). The main targeted missions of the RACER are: Search & Rescue, Emergency Medical Services, Passenger transport and Public/Parapublic. First flight of the rotorcraft is targeted by the end of 2022. Some pictures of the RACER are given in Figure 12 As designed in a European funded research program, the development leveraged on many partnerships. Regarding acoustics, this context allowed for various fruitful collaborations with research centers such as ONERA, DLR and IAG [17–20].

Figure 12: The RACER concept.

The RACER was originally based on the X3 [21] demonstrator but features many additional innovative characteristics (box-wing concept, optimized propellers, H-tail design...) in the range of aerodynamics and/or aeroacoustics. Noise minimization was considered from the beginning in the project. A particular attention was paid to the propeller's design and installation, leading to significant improvement with respect to the original X3 design. Moreover, a unique ability of the RACER, thanks to the introduction of an additional degree-of-freedom in its flight mechanics, holds a major effect in terms of main rotor noise emission. On the RACER configuration, part or totality of the propulsion can be ensured by the propellers, as illustrated on Figure 13. Therefore, setting the amount of mean propeller thrust provides control over α_{TPP}, unlikely to conventional helicopters. In addition, attitude control is provided by the horizontal stabilizer. This directly influences the vortices miss-distances and thus brings another control to move the main rotor blades away from their own wake and avoid BVI conditions.

This new configuration was analysed using the ONERA HMMAP tool-chain, whose functionning is illustrated in Figure 14. This comprehensive computation chain is

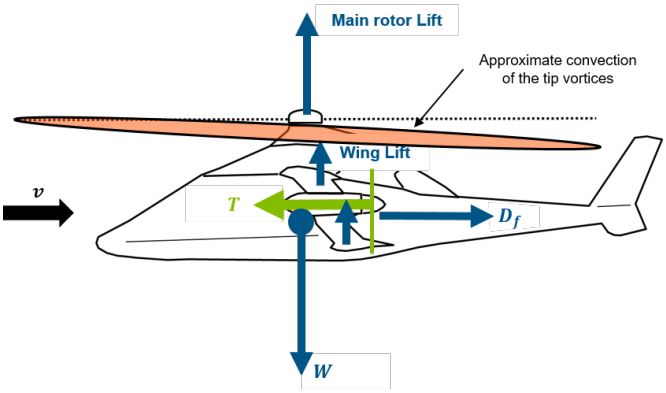

(a) Approximate longitudinal balance of the RACER for high thrust setting.

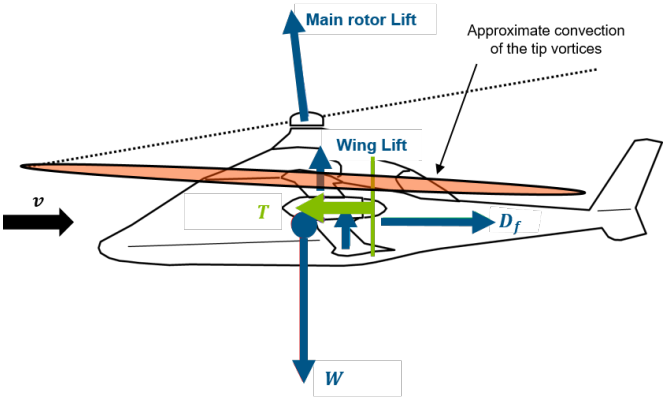

(b) Approximate longitudinal balance of the RACER for low thrust setting.

Figure 13: Approximate equilibrium of the new vehicle configuration for two different propeller thrust settings in cruise flight condition.

based on the HOST solver [22] and has been developed by ONERA in the 1990's [23]. Numerous improvements have been implemented since then, such as recent ones regarding BVI modelling in the frame of the French national-funded CHARME project [24]. This last feature is currently in use in Airbus Helicopters working environment.

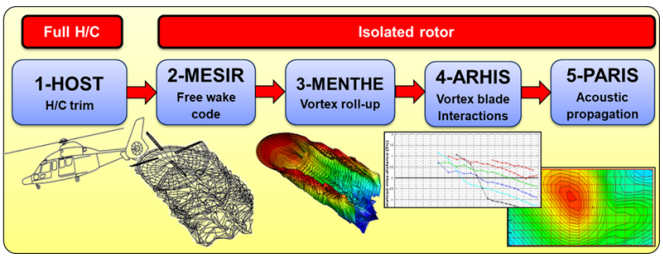

Figure 14: The HMMAP main rotor noise computation chain, courtesy of ONERA.

Figure 15 represents back-propagated far-field noise hemispheres, as the output of the HMMAP computation chain, for a cruise flight condition at 164 kt. The noise hemisphere on the left is representative of a high propeller thrust setting, resulting in a 'flat rotor'. Main rotor blade tip vortices are still convected a bit due to the induced velocity field, as shown on Figure 13a. The central hemisphere results from the computation for the main rotor operated with a positive longitudinal cyclic input, thanks to the RACER incidence control. The pitch attitude of the fuselage remains the same. The right picture represents the noise hemisphere for a main rotor operated with the same longitudinal cyclic input than for the central hemisphere, but with an additional positive fuselage pitch angle. A significant noise reduction from left to right is observed, highlighting the beneficial effect of main rotor "nose-down" incidence. It is also observed that the directivity patterns of the three noise hemispheres are quite similar. This is due to the fact that the epicycloidal vortex wake pattern stays mostly unchanged, as only the miss-distances are affected by the change of incidence. Such significant results are yet to be tempered, as it is known that numerical studies tend to return overestimated trends. The efficiency of such a noise reduction will be deeply investigated in the upcoming flight test campaign.

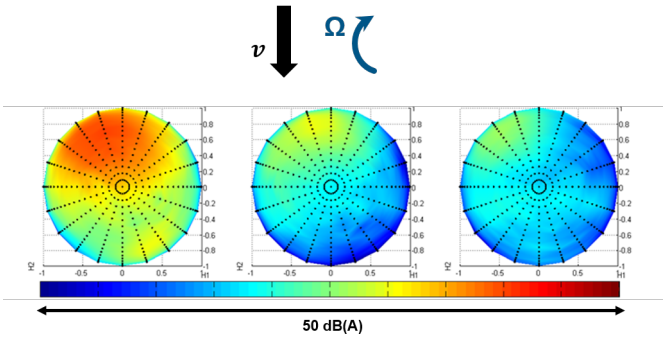

Figure 15: Influence of incidence control on main rotor noise hemispheres in moderate speed cruise condition (164 kt).

The effectiveness of incidence control was also checked for other flight conditions such as higher speed cruise, take-off and in particular approach, which is usually prone to BVI on conventional helicopters. Assessing if BVI can be avoided on the whole flight domain leads to a significant matrix of computations, which is currently being processed. It can be helped using first-order model based on simplified aeromechanics and Froude theory. This allows to get a rough estimate of the incidence domain to be avoided depending on vehicle airspeed and flight path angle. It can be shown that at low speed, due to the strong induced velocity and relatively weak advancing speed, BVI occurs only for high "nose-up" main rotor incidence values. With increasing speed, the induced velocity drops and the relative wind raises, thus

the incidence zone to be avoided holds much lower values. As the lever to control the main rotor incidence is mainly based on propeller mean thrust, it must also be ensured that the propeller noise remains at acceptable level. This is ensured using the CONCERTO computation chain, which provides an estimate of the propeller noise emission at an acceptable computational cost, accounting also for interaction effects such as wing-propeller interactions and main rotor-propeller interactions [20].

An ambitious flight test campaign dedicated to the acoustic characterization of the RACER, taking into account the results of the numerical study, is planned. It will allow the construction of a hemisphere database as illustrated in Figure 5. The optimization process described previously will then be applied. The expected output of the process is the capability of designing low noise procedures dedicated to the RACER, including the benefit of incidence control, on the top of the gains already demonstrated for conventional helicopters.

In view of the operational implementation of such procedures, in order to accurately follow the prescribed route in terms of lateral and vertical guidance and optimized incidence, the NAFTI project was put in place. The main NAFTI objective is to develop, manufacture, test and qualify up to safe for flight status a Flight Management System (FMS) with noise abatement functionality [25]. The complete avionics suite (including the FMS and the AFCS[1]) will support all capabilities of the flight management and guidance system that is in use on current helicopters plus an additional plug-in for specific complex low noise trajectories.

CONCLUSION

Reducing the population exposure to the noise associated to rotorcraft operations is needed as aviation is heading towards more sustainability. In this way, the special characteristics of rotorcraft noise emission are introduced. A good understanding of these mechanisms allows to build rotorcraft noise models and define new quieter ways of flying. First, an accurate noise footprint computation chain (CAROT), which allows to perform realistic environmental impact assessment, is presented. It can be used to support operators and local authorities to evaluate the population exposure to the noise generated by rotorcraft traffic. A better understanding of such impact is a first step towards more sustainable operations. Furthermore, CAROT can be embedded in a dedicated optimization algorithm that aims at computing rotorcraft low noise trajectories minimizing their impact on population. Important noise reduction can be obtained by flying such low noise procedures.

New rotorcraft configuration can bring additional degree-of-freedom in the optimization. Indeed, the ability to control incidence on the RACER can have a significant impact on noise reduction, as it allows control on the emission effect. Therefore, it makes it easier to design dedicated optimal low noise trajectories in terms of rate-of-descent and airspeed, without being constrained by the occurrence of BVI, as for conventional helicopters. For the RACER, the aggregation of the acoustic gains, obtained by the incidence control and the new low noise trajectories, can lead to more sustainable rotorcraft operations by reducing their noise impact on population.

ACKNOWLEDGMENTS

The authors wish to acknowledge the Clean Sky 2 Joint Undertaking (CSJU) for the financial support of this research performed in the frame of the Fast RotorCraft RACER project.

REFERENCES

[1] WHO. Environmental Noise Guidelines for the European Region. Technical report, WHO Regional Office for Europe, 2018.

[2] P. Rauch, M. Gervais, P. Cranga, A. Baud, J.-F. Hirsch, A. Walter, and P. Beaumier. Blue Edge™: The Design, Development and Testing of a New Blade Concept. In *American Helicopter Society 67th Annual Forum*, Fairfax, VA, 2011.

[3] F. Guntzer, V. Gareton, J.-P. Pinacho, and J. Caillet. Low Noise Design and Acoustic Testing of the Airbus Helicopter H160-B. In *45th European Rotorcraft Forum*, Warsaw, Poland, September 2019.

[4] Sharon L. Padula, Casey L. Burley, D. Douglas Boyd Jr., and Michael A. Marcolini. Design of quiet rotorcraft approach trajectories. NASA TM 215771, NASA, 2009.

[5] Frédéric Guntzer, Vincent Gareton, Marc Gervais, and Philippe Rollet. Development and testing of optimized Instrument Flight Rules (IFR) noise abatement procedures on EC155. In *American Helicopter Society 70th Annual Forum*, May 2014.

[6] Robert Morris, Matthew Johnson, K. Brent Venable, and James Lindsey. Designing noise-minimal rotorcraft approach trajectories. *ACM Transactions on Intelligent Systems and Technology*, 7(4):1–25, 2016.

[7] Eric Greenwood. Dynamic replanning of low noise rotorcraft operations. In *American Helicopter Society 75th Annual Forum*, May 2019.

[1] AFCS: Automatic Flight Control System

[8] P. Dieumegard, F. Guntzer, J. Caillet, and S. Cafieri. A Realistic Rotorcraft Noise Footprint Computation for Low-Noise Trajectory Optimization. In *Vertical Flight Society 78th Annual Forum*, Fort Worth, TX, May 2022.

[9] A. Le Duc, P. Spiegel, F. Guntzer, M. Lummer, H. Buchholz, and J. Götz. Simulation of Complete Helicopter Noise in Maneuver Flight using Aeroacoustic Flight Test Database. In *American Helicopter Society 64th Annual Forum*, Montreal, Canada, 2008.

[10] E. Greenwood, F. H. Schmitz, and R. D. Sickenberger. A Semiempirical Noise Modeling Method for Helicopter Maneuvering Flight Operations. *Journal of the American Helicopter Society*, 60(2):1–13, 2015.

[11] M. Gennaretti, J. Serafini, M. Molica Colella, and G. Bernardini. Simulation of helicopter noise in maneuvering flight. In *40th European Rotorcraft Forum*, September 2014.

[12] F.H. Schmitz. Reduction of Blade-Vortex Interaction (BVI) noise through X-force control. *Journal of the American Helicopter Society*, 43:14–24, January 1998.

[13] Bruitparif. Cartes stratégiques de bruit. `https://carto.bruitparif.fr/`, 2017. Online; accessed 28-July-2022.

[14] Charles Audet and J. E. Dennis. Mesh Adaptive Direct Search Algorithms for Constrained Optimization. *SIAM Journal on Optimization*, 17(1):188–217, 2006.

[15] Lucas Janson, Edward Schmerling, Ashley Clark, and Marco Pavone. Fast marching tree: A fast marching sampling-based method for optimal motion planning in many dimensions. *The International Journal of Robotics Research*, 34(7):883–921, 2015.

[16] P. Dieumegard, S. Cafieri, D. Delahaye, and R.J. Hansman. Using surrogates in black-box optimization for low-noise rotorcraft trajectory design. *Optimization and Engineering*, Under review.

[17] C. Oehlre, F. Frey, J. Thiemeier, M. Kessler, and E. Kraemer. Coupled and Trimmed Aerodynamic and Aeroacoustic Simulations for Airbus Helicopters's Compound Helicopter RACER. In *American Helicopter Society Technical Conference on Aeromechanics Design for Transformative Vertical Flight*, 2018.

[18] J. Yin, T. Schwarz, M. Wentrup, and F. Guntzer. DLR analysis on the noise emission from the racer configuration. In *45th European Rotorcraft Forum*, Warsaw, Poland, September 2019.

[19] J. Decours, J. Bailly, B. Ortun, S. Canard-Caruana, Y. Delrieux, R. Fukari, and F. Guntzer. RACER aero-acoustic propeller analysis and design. In *American Helicopter Society 75th Annual Forum*, Philadelphia, PA, 2019.

[20] G. Reboul, J. Bailly, P. Rottmann, L. Bekemeyer, G. Einarsson, and F. Guntzer. Prediction of RACER's Lateral Rotor Noise Using the CONCERTO Chain. In *American Helicopter Society 77th Annual Forum*, 2021.

[21] Douglas Nelms. Aviation Week Flies Eurocopter's X3. *Aviation Week & Space Technology*, July 2012.

[22] B. Benoit, A.-M. Dequin, K. Kampa, W. Gruenhagen, P.-M. Basset, and B. Gimonet. HOST: a general helicopter simulation tool for Germany and France. In *American Helicopter Society 56th Annual Forum*, Virginia Beach, VA, May 2000.

[23] P. Beaumier and Y. Delrieux. Description and validation of the ONERA Computational Method for the Prediction of Blade-Vortex Interaction Noise. *Aerospace Science and Technology*, 9:31–43, 2005.

[24] G. Reboul and F. Falissard. On the Use of CFD for improvement of Low-Fidelity Blade-Vortex Interaction Prediction Code. In *American Helicopter Society 75th Annual Forum*, Philadelphia, PA, 2019.

[25] T. Todd. Plan for Dissemination and Exploitation for the NAFTI project. Technical Report P1703N-SDRL-TSCU-3045-01.01A, European Commission, September 2020.